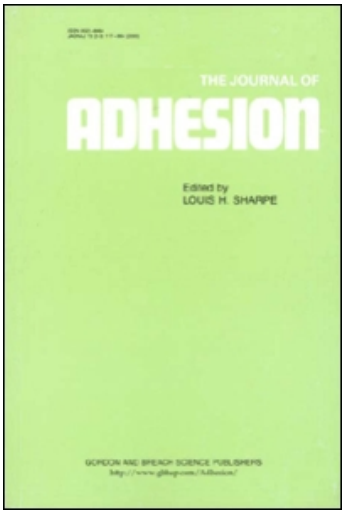

The Journal of Adhesion

Publication details, including instructions for authors and subscription information:
http://www.informaworld.com/smpp/title~content=t713453635

Adhesion and Removal of Particles from Surfaces Under Humidity Controlled Air Stream

Jérôme Cardot[a]; Nadège Blond[a]; Philippe Schmitz[a]
[a] UMR CNRS/INP-UPS 5502, Institut de Mécanique des Fluides de Toulouse, Toulouse, France

To cite this Article Cardot, Jérôme , Blond, Nadège and Schmitz, Philippe(2001) 'Adhesion and Removal of Particles from Surfaces Under Humidity Controlled Air Stream', The Journal of Adhesion, 75: 3, 351 — 368
To link to this Article: DOI: 10.1080/00218460108029609
URL: http://dx.doi.org/10.1080/00218460108029609

J. Adhesion, 2001, Vol. 75, pp. 351 - 368
Reprints available directly from the publisher
Photocopying permitted by license only

Adhesion and Removal of Particles from Surfaces Under Humidity Controlled Air Stream*

JÉRÔME CARDOT, NADÈGE BLOND and PHILIPPE SCHMITZ†

Institut de Mécanique des Fluides de Toulouse, UMR CNRS/INP-UPS 5502, Allée du professeur Camille SOULA, 31400 Toulouse, France

(Received 25 May 2000; In final form 5 October 2000)

The adhesion and the removal of individual micrometer-sized particles on a plane substrate are studied using an air shear flow cell. Laminar isothermal compressible flow characterization enables us to analyze the effect of various parameters such as particle size, air humidity, surface nature and surface charge on the aerodynamic forces required to remove the particles from the substrate. The results show that the increase of humidity (up to a critical value) favors particle removal when particles adhere under strong electrostatic forces on a non-conductive charged substrate. On the contrary, the existence of a capillary force disfavors particle removal beyond this critical humidity. The increase of the humidity disfavors the removal of particles in contact with an uncharged substrate. The results are interpreted in terms of a global adhesion force using a force and torque balance on a single particle in contact with a plane substrate. Moreover, the use of a high-speed video recording system enables us to determine the particle removal mechanisms as a function of the particle Reynolds number.

Keywords: Particle; Adhesion; Removal; Electrostatic; Air; Humidity

1. INTRODUCTION

The adhesion and the removal of micrometer-sized particles on solid surfaces under an air stream is encountered in many industrial

* Presented in part at the 23rd Annual Meeting of The Adhesion Society, Inc., Myrtle Beach, South Carolina, USA, February 20 - 23, 2000.

† Corresponding author. Tel.: 33-5-61-28-58-77, Fax: 33-5-61-28-58-78, e-mail: schmitz@imft.fr

applications, such as surface decontamination and gas filtration. The adhesion of very small particles is influenced by several complex phenomena such as Van der Waals attraction, electrostatic effects and capillary condensation [1, 2]. The Van der Waals force is due to the interactions between the molecules of the particle and the substrate. It can be calculated theoretically by the addition of the elementary contribution of all the molecular interactions, using the classical assumption due to Hamaker. The expression of the Van der Waals force depends on geometric parameters such as the particle radius, the separation distance, the contact area and on the Hamaker constant which is related to the physical properties of the bodies and of the fluid [3, 4]. In particular, it can be noticed that the Hamaker constant is about ten times lower in water than in air [5]. Thus, it can be expected that the Van der Waals effect can be reduced in the presence of water molecules on the surfaces as is the case in humid environments. The electrostatic effects are due to the surface nature and charges of the particle and the substrate. Electrostatic forces, which consist of the image, the Coulomb and the DEP forces have been widely studied [2]. There has been much debate in the literature on the effect of patches of electrostatic charges randomly distributed in localized regions of the surfaces on the global adhesion force. In some cases, the contributions of the Van der Waals and the electrostatic forces become comparable in magnitude [6]. The capillary force appears as a strong adhesive force at high humidity. Indeed, liquid can condense between the particle and the substrate. The shape of the capillary meniscus and, then, the expansion of the liquid region under the particle depends on the humidity and on the particle/substrate system. A review of a number of works on humidity effects on adhesion [7] has shown a wide scatter of reported experimental data. The values of the capillary force can be determined numerically [8, 9] taking into account the contributions of the surface tension of the air/water interface and of the capillary pressure due to the curvature of the interface. The capillary force can drastically increase the global adhesion force depending on particle size. Capillary condensation can also contribute to an increase of the adhesion force due to the increase of the contact area and the deformation of the surfaces [10].

Many experimental studies on particle adhesion on surfaces have already been carried out using different techniques to remove particles previously deposited, such as centrifugation [11], vibrations [12],

impacting [13], electrostatic field [14, 15], and fluid mechanics [16–19]. Indirect techniques using fluid flow to remove particles are very interesting because they are close to the cleaning processes of surfaces and filters. The associated studies focus on the global fluid flow conditions necessary to dislodge particles from the surface. While the flow is laminar in liquids, air flow is generally turbulent [16, 20]. It is true that in most applications the air flow is turbulent. However, even if turbulent flow can generate strong wall shear stress, it also produces unsteady events near the wall, called bursts. Due to these unsteady and unpredictable events, it is generally complicated to interpret particle removal and, therefore, it is quite difficult to characterize the effect of the different particle-surface interactions on particle adhesion. The objective of the present paper is to analyze the particular effect of air humidity on particle adhesion and removal for different particle sizes and for surfaces of different nature. To this end, a well-defined, laminar, high air shear flow is used to determine the wall shear stress necessary to remove individual particles from a surface. In this method, the air flow close to the wall can be assumed to be a non-inertial flow, *i.e.*, Stokes flow. This allows us to make use of the well-known expressions for the aerodynamic forces and torque which apply on a single spherical particle in contact with a plane under linear shear flow [21–23]. An analog shear flow cell has already been successfully employed in aqueous media to study particle/membrane interactions in cross-flow microfiltration [18] and the effect of fibrin bio-polymer layers on platelet removal [19]. The results are interpreted in terms of a global adhesion force using a force and torque balance on a single particle in contact with a plane. Moreover, the use of a high-speed video recording system enables us to determine the particle removal mechanisms as a function of the particle Reynolds number.

2. EXPERIMENTAL

2.1. Device and Materials

The laminar air flow is pressure driven using a vacuum pump and a flow regulator located downstream from the shear flow cell. The humidity and temperature are controlled using a climatic enclosure located upstream from the shear flow cell. The shear flow cell is

mounted on the stage of an inverted microscope (NIKON Diaphot), coupled to a CCD camera with a video image processing system for visualization and counting of particles, Figure 1. The cell is specially designed to reach high laminar shear rates ($\gamma = 1.2 \times 10^6 s^{-1}$). It is composed of a bottom glass plate (450×70 mm) and an upper Plexiglas^{TM} plate of the same dimensions pierced for the entry and exit of fluid and for a pressure tap, Figure 2. These plates are separated by

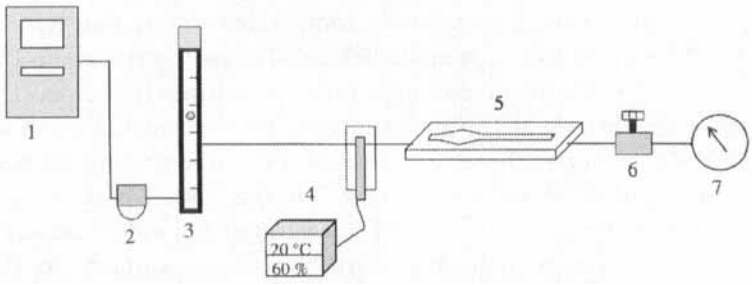

1: Climatic enclosure
2: Filter
3: Flowmeter
4: Temperature and Hygrometry measurement
5: Air shear flow cell under microscope
6: Regulation flow gate
7: Vacuum pump

FIGURE 1 Experimental device.

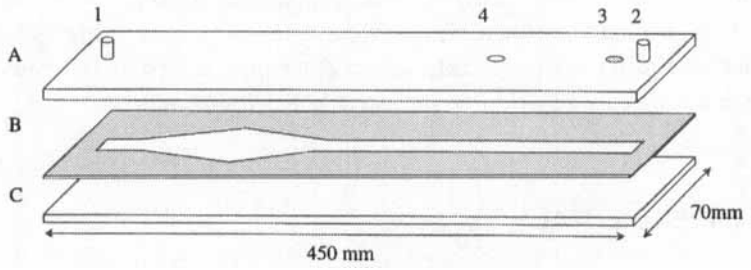

1: Entry of fluid
2: Exit of fluid
3: Pressure tap
4: Particles deposit

A: Plexiglas plate
B: Flow canal (h:300 µmxl:1 cm)
C: Glass plate

FIGURE 2 Air shear flow cell.

a hollowed-out steel plate (thickness 0.3 mm) for channeling the fluid flow. All the plates are held together with aluminium clamps. The rectangular flow channel (10 mm width) follows a diverging-converging channel, in order to ensure a uniform flow at the entrance of the region of interest. The observation area of particle removal is located far downstream from the rectangular channel entry where a laminar Poiseuille flow is established. Therefore, it can be assumed that the particles deposited in the observation area are submitted to a linear shear flow.

Spherical glass beads (21 or 37 μm diameter, supplied by Whitehouse Scientific Ltd) are used as models of real particles.

2.2. Flow Characteristics

The dimensions of the air shear flow cell are chosen to obtain a fully-developed laminar flow of high shear flow rate in the region where particles are deposited. However, the pressure drop through the cell being of the same order as the static pressure in the system, the air flow in the cell is compressible. Therefore, the governing equations for fully-developed laminar compressible flow, *i.e.*, the mass and momentum equations and the equation of state for perfect gases, are solved analytically using the viscous boundary layer assumption [24]. Then, the following expressions for the pressure, $p(x)$, volumetric mass, $\rho(x)$ and velocity, $u(x, y)$ along the channel are obtained:

$$\begin{cases} p(x) = \sqrt{(p_3^2 - p_4^2)\frac{x}{(x_3 - x_4)} + p_4^2} \\ \rho(x) = \frac{p(x)}{RT} \\ u(x,y) = \frac{3Q_m}{4h\rho(x)}\left(1 - \left(\frac{y}{h}\right)^2\right) \end{cases} \tag{1}$$

where Q_m is the mass flow rate, h is the half channel height, R the perfect gas constant, T the absolute temperature and p_3 and p_4 are two pressure values at x_3 and x_4 along the channel.

Finally, the mass flow rate can be expressed as follows:

$$Q_m = \frac{(p_4^2 - p^2)h^3\ell}{3\mu(x - x_4)RT} \tag{2}$$

where ℓ is the width of the channel.

The aerodynamics in the cell was carefully checked before making adhesion experiments. To this end, pressure drop measurements were carried out. It was found that the experimental pressure drop as a function of the mass flow rate in the region of interest agreed very well with the quadratic variation given by the theoretical expression of Eq. (2) [24]. Therefore, Eq. (2) shows that the knowledge of the static pressure, p_4, at x_4 along the channel and the mass flow rate, Q_m, enables us to determine the static pressure, p, and then the volumetric mass, ρ, and the humidity, H, everywhere in the cell and, in particular, close to the particles, during the experiments. Using the expression for $u(x,y)$ of Eq. (1), the corresponding wall shear stress can be expressed as:

$$\tau_p = \frac{3\mu Q_m}{2h^2 \ell \rho} \tag{3}$$

2.3. Method of Operation

First, the three plates (glass plate, Plexiglas™ plate and hollowed-out steel plate) are carefully cleaned using a pure alcohol solution. Therefore, the surfaces are not electrostatically charged. Second, the particles are deposited on the bottom plate far from the entrance region of the channel using a metallic needle. This deposition technique is difficult to employ because the glass beads have to be roughly uniformly deposited with respect to a mean separation distance between particles of about five times the particle diameter or greater. This separation distance was chosen to minimize artifacts caused by aerodynamic interactions between particles, such as shielding of the shear field. This allows us to assume that the theoretical expressions reported in the next section for the aerodynamic forces and torque given for a single particle are valid, as demonstrated numerically [25]. The aggregates of two particles or more which sometimes exist after the deposition procedure are not taken into account in the measurements. The flow rate is then increased step by step from zero to the maximum shear flow rate (a typical step is 5 minutes). The number of individual particles remaining at the surface is counted at the end of each step by

means of phase-contrast optical microscopy and image acquisition. Each experiment consists of about 100 particles previously deposited.

3. THEORETICAL MODEL

In order to understand the adhesion and removal mechanisms of a single spherical particle in contact with a plane in a linear shear flow, a force and torque balance on the particle is performed. The theory of aerodynamic effects which applies on a spherical particle under low inertial shear flow is used [21–23], Figure 3. The expressions for the corresponding drag force, F_D, lift force, F_L, and aerodynamic torque, C_Z, are the following:

$$\begin{cases} F_D = 6\pi\tau_p a^2 K_D & \tau_p = \mu\gamma \\ C_Z = 0.38 a F_D \\ F_L = K_L \tau_p a^2 \mathrm{Re}_p \end{cases} \tag{4}$$

Here a is the radius of the particle, τ_p is the wall stress, μ and ν are the dynamic and kinetic viscosities of air, respectively. K_D and K_L are the

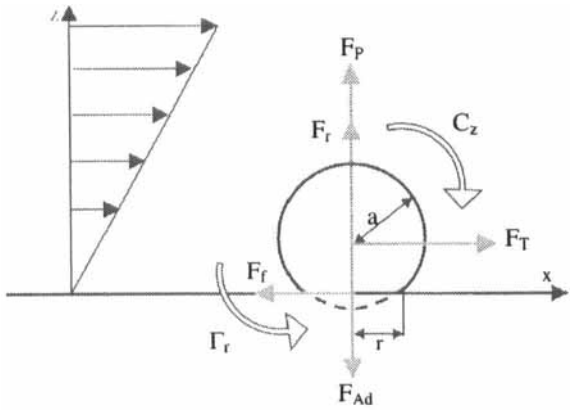

FIGURE 3 Forces and torque on a single particle in contact with a plane submitted to a linear shear flow.

correction factors in the case of a single particle in contact with a plane. Re_p is the particle Reynolds number. For convenience, the velocity of the fluid at the particle location is replaced by $a\tau_p/\mu$ as can be seen in Eq. (4), assuming a linear velocity profile close to the particle as a/h is lower than 1. It can be noticed that the particle Reynolds number is supposed to be greater than zero but low with respect to the assumption of low inertial flow close to the wall, *i.e.*, close to the particles. However, the expression for the lift force is extrapolated to Re_p of the order of 1.

The model of contact is based on the dry friction law between the particle and the surface. The contact area is a disk of unknown radius r. Therefore, a friction force, F_F, related to the static friction coefficient, f_0, and a friction torque at the contact point, Γ_F, related to the rolling friction coefficient, g_0, has to be considered in the balance, as can be seen in Figure 3. Finally, the model previously described allows us to determine the critical wall shear stress, τ_p, required to overcome the global adhesion force, F_{Ad}, for the different removal mechanisms which can occur (rolling, τ_{PR}, sliding, τ_{PS}, and lifting, τ_{PL}) using the values of K_D and K_L given in the literature [22,23]. The three critical wall shear stresses can be evaluated by performing a balance of forces and torque [17,26] and using the expressions given in Eq. (4). If the removal mechanism is believed to be rolling, the total adhesion force can be obtained from the following torque balance:

$$C_Z + aF_D = g_0(F_{Ad} - F_L) \tag{5}$$

It can be noticed that the rolling friction coefficient, g_0, has the dimension of a length. The corresponding wall shear stress, τ_{PR}, can be deduced to give:

$$\tau_{PR} = \frac{g_0 F_{Ad}}{a^2(43.9a + 9.257 g_0 Re_p)} \tag{6}$$

If the removal mechanism is sliding, the total adhesion force can be obtained from the following force balance:

$$F_D = f_0(F_{Ad} - F_L) \tag{7}$$

The corresponding wall shear stress is obtained as:

$$\tau_{PS} = \frac{f_0 F_{Ad}}{a^2(32.00 + 9.257 f_0 \mathrm{Re}_p)} \tag{8}$$

If the removal mechanism is lifting, the total adhesion force can be obtained from the following force balance:

$$F_L = F_{Ad} \tag{9}$$

The corresponding wall shear stress is given by:

$$\tau_{PL} = \frac{F_{Ad}}{9.257 \mathrm{Re}_p a^2} \tag{10}$$

Let us now consider the three following ratios:

$$A = \frac{\tau_{PS}}{\tau_{PL}} = \frac{9{,}257 f_0 \mathrm{Re}_p}{32 + 9{,}257 f_0 \mathrm{Re}_p} \tag{11}$$

$$B = \frac{\tau_{PR}}{\tau_{PL}} = \frac{9{,}257 g_0 \mathrm{Re}_p}{43{,}9a + 9{,}257 g_0 \mathrm{Re}_p} \tag{12}$$

$$C = \frac{\tau_{PS}}{\tau_{PR}} = \frac{43{,}9a(f_0/g_0) + 9{,}257 f_0 \mathrm{Re}_p}{32 + 9{,}257 f_0 \mathrm{Re}_p} \tag{13}$$

It is clear that the two ratios A and B are always less than 1, meaning that the particles cannot be removed by a lifting mechanism. Nevertheless, it can be mentioned that an increase of the lift force leads to lower critical wall shear stresses τ_{PR} and τ_{PS}, which contributes to an easier removal by sliding or rolling mechanisms. The ratio C depends on the term $a(f_0/g_0)$. Keeping in mind that f_0 is lower than 1 and as the particle radius a is small (about 10 to 20 microns), it can be assumed that $a(f_0/g_0)$ is lower than 1. Subsequently, the experimental results will be interpreted in terms of global adhesion force between particle and surface assuming that particles leave the surface under a sliding mechanism as soon as the wall shear stress, τ_p, equals τ_{PS}. Then the expression of the global adhesion force can be obtained from Eq. (8) and written as follows:

$$F_{Ad} = \frac{a^2 \tau_{PS}(32 + 9.257 f_0 \mathrm{Re}_p)}{f_0} \tag{14}$$

4. RESULTS AND DISCUSSION

Experiments are performed at various humidity, surface characteristics and bead sizes. Various surfaces are used: a glass plate considered as an uncharged surface, and a Plexiglas^{TM} plate considered as a non-conductive, charged surface on which the surface charges are randomly distributed. The results are presented in the form of detachment curves which give the number of particles remaining in the observation area (expressed as percent of initial number of particles, N_0) as a function of the wall shear stress applied. Each curve is the mean curve of five experiments.

4.1. Effect of Air Humidity

The influence of air humidity on the removal of particles deposited on the uncharged glass plate is studied. The detachment curves are plotted for different local air humidity, in Figure 4 for the 21 μm glass beads and in Figure 5 for the 37 μm glass beads. As can be expected, the removal of the 37 μm glass beads is easier than the removal of the

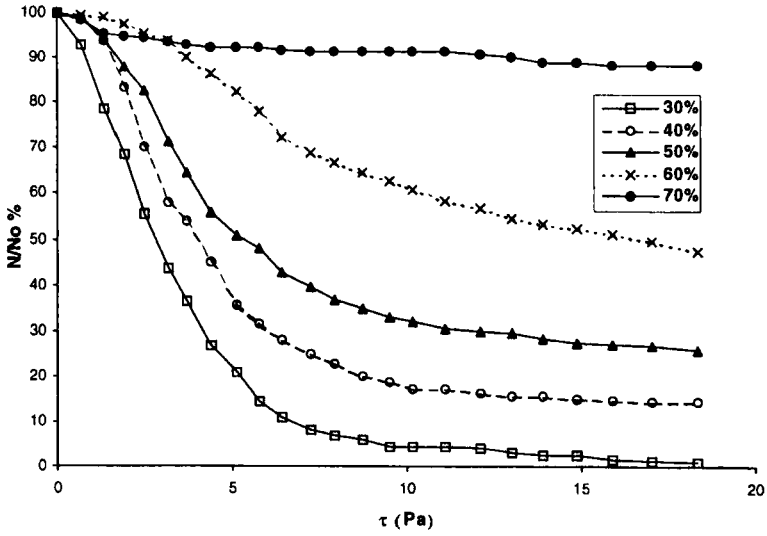

FIGURE 4 21 μm glass bead removal on a wettable glass surface for different humidity.

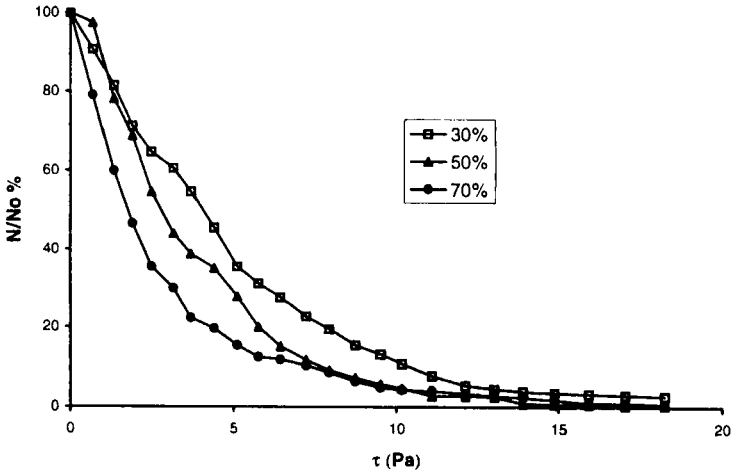

FIGURE 5 37 μm glass bead removal on a wettable glass surface for different humidity.

21 μm beads since the aerodynamic forces, F_D and F_L, are proportional to a^2. For the 21 μm beads, the increase of humidity disfavors particle removal due to the existence of molecular adsorption on the glass surfaces leading to the capillary condensation mechanism under the particles. Thus, the subsequent capillary force strongly increases the global adhesion force that prevents particle removal beyond a relative humidity of about 60%. This value agrees with the range 60% – 90% of the critical humidity above which adhesion increases due to a change in the bonding mechanism, from that of an adsorbed layer to a liquid bridge, obtained for various particle/substrate systems and surface treatments [7]. It can be seen that the maximum wall shear stress of 18 Pa, corresponding to a drag force, F_D, of 6.3×10^{-8} N and a lift force, F_L, of 7.8×10^{-8} N, is not sufficient to remove the particles for a humidity of 70% (less than 10% of particles are removed). Using the theoretical model, assuming that the other effects can be neglected relative to the capillary effect at high humidity, and taking a friction coefficient, f_0, equal to 0.1 as an approximate value for a glass/glass contact, it can be deduced that the adhesive capillary force is higher than 10^{-7} N. On the contrary, the capillary force appears to be negligible for the 37 μm glass beads since particle removal is facilitated when the humidity increases, as can be seen in Figure 5. The capillary

meniscus which forms with under the particle at high humidity is smaller relative to particle size compared 20 μm glass beads, which can explain the relatively low intensity of the capillary force. Therefore, the other forces which can modify the total adhesion force as the humidity varies are the Van der Waals' and electrostatic forces. First, it can be noticed that the Hamaker constant which appears in the theoretical expression for the Van der Waals force is lower in liquids than in gases [5]. Consequently, the increase of the humidity can lead to the decrease of the Van der Waals force due to the existence of water molecule adsorption and capillary condensation under the particle in the contact area. Second, residual patches of weak charges on the surfaces can be more uniformly distributed when the water molecule adsorption occurs, which contributes to the decrease of the electrostatic force. These phenomena can explain why the results plotted in Figure 5 show that the total adhesion force is reduced as the humidity increases.

4.2. Effect of Surface Wettability

The following experiments are done with the 21 μm glass beads. The uncharged glass plate is coated with a $(CF_2)_n$ layer (supplied by Saint-Gobain) to obtain a non-wettable surface, thus allowing us to study the effect of surface wettability on the existence of capillary condensation. Figure 6 shows that particle removal is much easier in the whole range of humidity. In order to estimate the global adhesion force, the wall shear stress required to remove 50% of particles is taken as the critical wall shear stress, τ_{PS}. Thus, the theoretical model can be applied using the assumption of sliding removal. Here the friction coefficient, f_0, for the glass/coated glass contact is kept equal to 0.1 (glass/glass contact case) even if it should be lower. The calculated global adhesion force of the particles between the two cases, wettable surface and non-wettable surface, obtained using the expression of Eq. (14), are reported in Table I. For convenience, the ratio of the calculated global adhesion force divided by the calculated global adhesion force, $F_{Ad\ nm}$, obtained for the best removal conditions (non-wetting, 30% humidity) are reported in the right hand column. It can be seen that an appropriate treatment of the surface can reduce the global adhesion force by a factor of 50 for a high humidity of 70%.

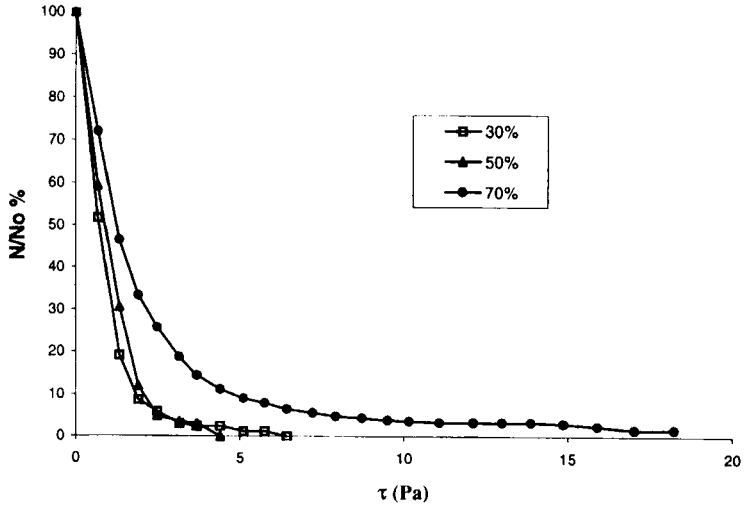

FIGURE 6 21 μm glass bead removal on a non-wettable glass surface for different humidity.

TABLE I Global adhesion force intensity for wettable and non-wettable surfaces for different humidity

Surface wettability	*Air humidity* (%)	*Adhesion force* (*N*)	*Adhesion force*/$F_{Ad\ nm}$
Wettable	30%	1.29×10^{-08}	5
	50%	2.53×10^{-08}	9.9
	70%	1.39×10^{-07} (88%)	> 54
Non-wettable	30%	$F_{Ad\ nm} = 2.57 \cdot 10^{-09}$	1
	50%	2.84×10^{-09}	1.1
	70%	3.7×10^{-09}	1.4

4.3. Effect of Surface Charge

Experiments are performed with 21 μm glass beads adherent to the non-conductive Plexiglas™ plate previously charged by triboelectricity. When the surface is charged, the particles in contact with the surface experience electrostatic forces of high magnitude, such as Coulomb and image forces [2]. The particle removal is studied for different humidity values as can be seen in Figure 7. Recall that the initial Plexiglas™ surface charge remains uncontrolled in this set of experiments. Indeed, the surface charges are not uniformly distributed

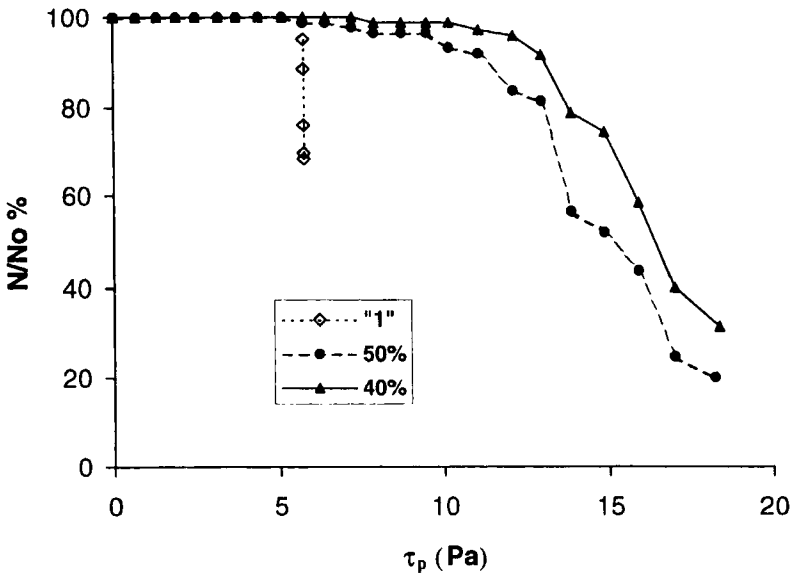

FIGURE 7 21 μm glass bead removal on a charged surface for different humidity.

since the Plexiglas™ surface is a non-conductive surface. Therefore, it is not possible to obtain good reproducibility. However, the results clearly show the existence of a significant critical wall shear stress below which the particles remain attached to the surface. This phenomenon is easily explained by the strong adhesion forces experienced by the particles. Moreover, it can be expected that the higher the surface charge, the higher the critical shear stress. Unfortunately, the present experiments do not allow us to verify this idea since the surface charge is not controlled.

The effect of air humidity on particle removal is presented in Figure 8. First, the wall shear stress is kept constant from the beginning of particle removal, which corresponds to a low humidity of 30% (5 Pa). Then the humidity is increased from 30% to 80%. Finally, the wall shear rate is increased again (see the corresponding curve designated "1" in Fig. 7). The increase of the humidity facilitates particle removal until a critical value (about 50%) beyond which the capillary force becomes dominant. Molecular adsorption increases the surface conductivity as the humidity increases, allowing for a more uniform distribution of the surface charges. Then the local surface

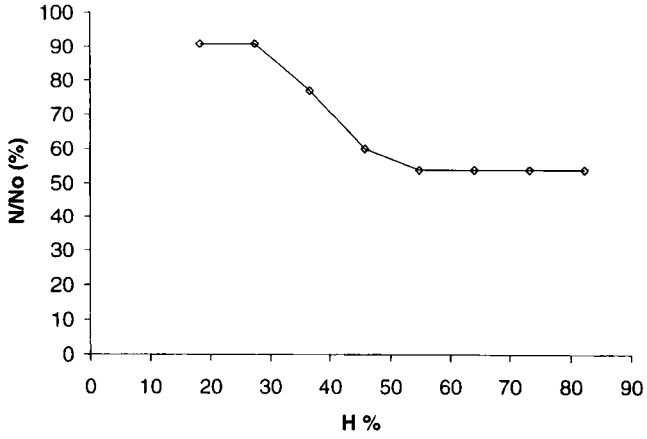

FIGURE 8 Influence of air humidity on 21 μm glass beads removal on a charged surface at constant shear stress.

charge experienced by particles is reduced, thus, decreasing the magnitude of the attractive electrostatic forces.

5. PARTICLE REMOVAL MECHANISMS

In order to analyze carefully the removal mechanisms of single spherical particles in contact with a plane in a linear shear flow (rolling, sliding or lifting), a high-speed video recording system (1000 images per second) is used. Particles of 21 μm and 37 μm are observed at various flow rates which correspond to various particle Reynolds number in order to visualize the different removal mechanisms.

First, it is seen that some particles can have a tiny motion without being removed at very low particle Reynolds numbers ($Re_p \ll 1$). If they are removed, they strike other particles deposited some diameters further away, Figure 9a. At this stage, the rolling or sliding removal mechanisms may be balanced by an obstacle (roughness or dirt) in some cases. Second, for $Re_p \sim 1$ some collisions can be sometimes observed, but generally a removed particle does not strike another particle remaining attached, Figure 9b. Thus, it is confirmed that the lift aerodynamic force is significant even if the main removal force acting on the particle is still the drag force. Third, at a higher particle

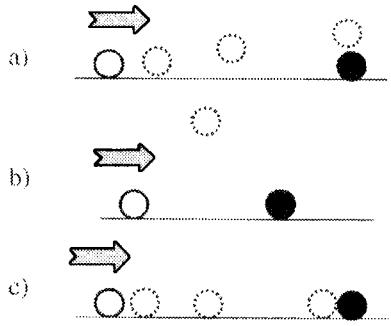

FIGURE 9 Particle removal mechanisms for different particle Reynolds numbers; (a) $Re_p \ll 1$, (b) $Re_p \sim 1$, (c) $Re_p \sim 10$.

Reynolds number ($Re_p \sim 10$ or higher), the particles are still removed by the rolling or sliding mechanisms but the lift force is dominant as soon as they move. Indeed, it is seen that they do not strike any other particles after removal, Figure 9c. Furthermore, it can be noticed that the motion is very fast at this stage, then the observation of particle removal mechanisms becomes quite difficult.

6. CONCLUSION

An experimental device has been developed and applied to study the adhesion and the removal of particles from surfaces under a humidity controlled air stream. The effects of humidity, surface characteristics (charge, wettability) and particle size have been evidenced and explained. It was shown that a capillary force appears at high humidity. This capillary force does not exist for the bigger particles (37 μm) or in the case of a non-wettable surface. Increasing the humidity favors particle removal in the case of a non-conductive charged surface until the capillary force appears. Moreover, the observation of particle removal enabled us to identify different removal mechanisms related to the particle Reynolds number. Further studies using a controlled charge surface will allow us to perform a quantitative analysis of the effect of the surface charge on particle adhesion and removal.

References

[1] Krupp, H., *A Theoretical Review of Particle Adhesion* (Plenum Press, New York, 1988), p. 129.
[2] Jones, T. B., *Electromechanics of Particles* (Cambridge University Press, 1995).
[3] Elimelech, M., Gregory, J., Jia, X. and Williams, R., *Particle Deposition and Aggregation: Measurement, Modelling and Simulation* (Butterworth Heineman, Oxford, 1995).
[4] Visser, J., *Adhesion of Colloidal Particles*, Surface and Colloid Science (John Wiley and Sons, New York, 1976).
[5] Israelachvili, J., *Intermolecular and Surface Forces* (Academic Press, London, 1992).
[6] Gady, B., Quesnel, D. J., Rimai, D. S., Leone, S. and Alexandrovich, P., "The adhesion of irregularly shaped particles: Effects of Van der Waals forces and electrostatically charged patches", *Proceedings of the 22nd Annual Meeting of the Adhesion Society* (1999), p. 22.
[7] Harnby, N., Hawkins, A. E. and Opalinski, I., "Measurement of the adhesion force between individual particles with moisture present", *Trans IchemE* **74**, 605 (1996).
[8] Orr, F. M. and Scriven, L. E., "Pendular rings between solids: meniscus properties and capillary force", *J. Fluid Mech.* **67**, 723 (1975).
[9] Joseph, P., Zasadsinski, A. N., Sweeney, J. B., Davis, H. T. and Scriven, L. E., "Finite element calculations of fluid menisci and thin films in a model porous media", *J. Colloid Interf. Sci.* **119**, 108 (1987).
[10] Tang, J. and Busnaina, A. A., "The acceleration of adhesion induced deformation of PSL particles on silicon substrates due to capillary force", *Proceedings of the 23rd Annual Meeting of the Adhesion Society* (2000), p. 367.
[11] Zimon, A. D., *Adhesion of Dust and Powder* (Plenum Press, London, 1966).
[12] Derjaguin, V. and Zimon, A. D., "Adhesion of powder particles to plane surfaces", *Kalloidn Z.* **23**, 544 (1961).
[13] Otsuka, A., "Measurement of adhesive force between particles of powdered materials and a glass substrate by means of impact separation technique", *Chem. Pharm. Bull.* **32**, 741 (1988).
[14] Mizes, H. A., "Adhesion of small particles in electric fields", *J. Adhesion Sci. Technol.* **8**, 937 (1994).
[15] Hays, D. A., "Adhesion of charged particles", *J. Adhesion Sci. Technol.* **9**, 1063 (1995).
[16] Cleaver, J. W. and Yates, B., "Mechanism of detachment of colloidal particles from a flat substrate in a turbulent flow", *J. Colloid Interf. Sci.* **44**, 3 (1973).
[17] Sharma, M. M., Chamoun, H., Sita Rama Sarma, D. S. H. and Schechter, R. S., "Factors controlling the hydrodynamic detachment of particles from surfaces", *J. Colloid Interf. Sci.* **149**, 121 (1992).
[18] Elzo, D., Schmitz, P., Houi, D. and Joscelyne, S., "Measurement of particle/membrane interaction by a hydrodynamic method", *J. Membrane Sci.* **109**, 43 (1996).
[19] Lorthois, L., Schmitz, P., Houi, D. and Angles Cano, E., "Experimental study of fibrin embolization under shear flow", *J. Adhesion* **72**, 229 (2000).
[20] Soltani, M. and Ahmadi, G., "Detachment of rough particles with electrostatic attraction from surface in turbulent flow", *J. Adhesion Sci. Technol.* **13**, 325 (1999).
[21] O'Neill, M. E., "A sphere in contact with a plane wall in a slow linear shear flow", *Chem. Eng. Sci.* **23**, 1293 (1968).
[22] Krishnan, G. P. and Leighton, D. T., "Inertial lift on a moving sphere in contact with a plane wall in a shear flow", *Phys. Fluids* **7**, 2538 (1995).

[23] Leighton, L. A. and Acrivos, A., "The lift on a small sphere touching a plane in the presence of a simple shear flow", *Z. Agnew. Math. Phys.* **36**, 174 (1985).
[24] Cardot, J., *Adhésion et détachement de particules en contact avec une surface sous écoulement d'air, Ph.D. Thesis*, INPT, Toulouse, France (2000).
[25] Brooks, S. B. and Tozeren, A., "Flow past an array of cells that are adherent to the bottom plate of a flow channels", *Computers and Fluids* **25**, 741 (1996).
[26] Hubbe, M. A., "Theory of detachment of colloidal particles from flat surfaces exposed to flow", *Colloids and Surfaces* **12**, 151 (1984).